Polymer 49 (2008) 3091–3097

Contents lists available at ScienceDirect

Polymer

journal homepage: www.elsevier.com/locate/polymer

Free volume and permeabilities of O_2 and H_2 in Nafion membranes for polymer electrolyte fuel cells

Hamdy F.M. Mohamed [a,b,*], K. Ito [a], Y. Kobayashi [a], N. Takimoto [c], Y. Takeoka [c,d], A. Ohira [c]

[a] NMIJ, National Institute of Advanced Industrial Science and Technology (AIST), Central 5, 1-1-1 Higashi, Tsukuba, Ibaraki 305-8565, Japan
[b] Physics Department, Faculty of Science, Minia University, B.O. 61519 Minia, Egypt
[c] FC-Cubic, National Institute of Advanced Industrial Science and Technology (AIST), Tokyo 135-0064, Japan
[d] Department of Chemistry, Sophia University, 7-1 Kioi-cho, Chiyoda-ku, Tokyo 102-8554, Japan

ARTICLE INFO

Article history:
Received 27 December 2007
Received in revised form 15 April 2008
Accepted 2 May 2008
Available online 8 May 2008

Keywords:
Positron annihilation
Permeability
Nafion

ABSTRACT

The mechanism of gas permeation in Nafion membranes for polymer electrolyte fuel cells has been investigated from the viewpoint of free volume. Three different samples, a membrane with ionic exchange capacity (IEC) = 0.92 meq/g, and recast samples with IEC = 0.92 and 1.00 meq/g were used after drying. Free volume was quantified using the positron annihilation lifetime (PAL) technique and gas permeabilities were measured for O_2 and H_2 as functions of temperature and relative humidity. Good linear correlations between the logarithm of the permeabilities at different temperatures and reciprocal free volume indicate that gas permeation in dry Nafion is governed by the free volume. Nevertheless permeabilities are much smaller than the corresponding flexible chain polymer with a similar free volume size due to stiff chains of the perfluoroethylene backbone. In highly hydrated Nafion above 60% relative humidity, where the O_2 permeability varies oppositely to the free volume, gas permeation proved to be controlled by the gradual increase in overall flexibility of the Nafion–water system.

1. Introduction

To improve the power density and efficiency of polymer electrolyte fuel cells (PEFCs), polymer membranes with higher proton conductivity and lower gas permeability are desired. Nafion developed by the DuPont Company in the early 1970s displays remarkable properties as the membrane for PEFCs. It possesses high mechanical, thermal and chemical stability coupled with high ion conductivity and selectivity [1]. The polymer is a perfluorosulfonate resin in which hydrophilic perfluoroether side chains terminated with $-SO_3^-H^+$ groups are randomly distributed along the perfluoroethylene backbone (Fig. 1). The side chains are readily saturated by water and form clusters. In hydrated Nafion, the clusters are interconnected with each other, providing higher proton conductivity [2,3]. This cluster model has been supported by both theory [4] and experimental observations by various techniques [5,6].

Because of their importance for PEFCs, a number of studies have been conducted on diffusivity, solubility, and permeability of O_2 and H_2 in hydrated Nafion [7–12]. Most of the studies showed that for both O_2 and H_2 the solubility decreases but the diffusivity and permeability increase with increasing water uptake or relative humidity. These results have been discussed qualitatively on the basis of the cluster model by considering invariant aqueous (cluster) and hydrophobic perfluoroethylene phases, and the interface region. However, the gas diffusion and permeation in polymers are strongly dependent on free volume (subnanometer scale open space), so that the simple discussion based on the cluster model, without the consideration of the interaction between the aqueous and hydrophobic phases or the change of their nano-structures, is not satisfactory.

Positron annihilation lifetime (PAL) spectroscopy has established itself as a powerful probe for the characterization of free volume in polymers due to the unique property of a positronium (Ps) atom, the hydrogen-like bound state between a positron and an electron [13]. In polymers there exist three states of positrons characterized by lifetimes τ_1, τ_2, τ_3 and the corresponding relative intensities I_1, I_2, I_3, respectively: spin antiparallel *para*-positronium (*p*-Ps) with $\tau_1 \sim 125$ ps, a free positron with $\tau_2 \sim 450$ ps, and spin parallel *ortho*-positronium (*o*-Ps) with $\tau_3 \sim 1$–10 ns [13–23]. The lifetime τ_3 of *o*-Ps is determined by the overlap of its wave function with that of the electrons in the polymer. A smaller size of free volume holes facilitates larger overlap, and therefore, shorter lifetime [24]. The relationship between lifetime τ_3 and average radius R

* Corresponding author. NMIJ, National Institute of Advanced Industrial Science and Technology (AIST), Central 5, 1-1-1 Higashi, Tsukuba, Ibaraki 305-8565, Japan. Tel.: +81 29 861 4626; fax: +81 29 861 4622.
E-mail addresses: hamdyfm@link.net (H.F.M. Mohamed), y-kobayashi@aist.go.jp (Y. Kobayashi), a-oohira@aist.go.jp (A. Ohira).

0032-3861/$ – see front matter © 2008 Elsevier Ltd. All rights reserved.
doi:10.1016/j.polymer.2008.05.003

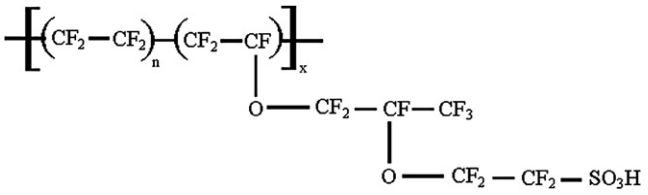

Fig. 1. Chemical structure of Nafion.

of free volume holes in spherical approximation is given by the Tao–Eldrup model [25,26] as

$$\tau_3 = 0.5\left\{1 - \frac{R}{R_o} + \frac{1}{2\pi}\sin\left(\frac{2\pi R}{R_o}\right)\right\}^{-1} \text{(ns)}, \quad (1)$$

where $R_o = R + \Delta R$ and $\Delta R = 0.166$ nm is the thickness of the homogenous electron layer in which the positron in *o*-Ps annihilates [27]. The free volume size $V_{FV,Ps}$ in nm^3 is calculable as

$$V_{FV,Ps} = 4\pi R^3/3. \quad (2)$$

The free volume hole size obtained by Eqs. (1) and (2) has been successfully applied to explain diffusion and permeation of various gases in polymers. Specifically good correlations were found between the diffusivities of Ar, O_2 and N_2, and $V_{FV,Ps}$ for such polymers as polydimethylsiloxane, polystyrene, polysulfone, polyethersulfone with relatively flexible backbones [28,29]. Different correlations of O_2 and N_2 diffusion coefficients were observed for fluorinated poly(amide imide), poly(ester imide) and polyimide with more rigid chains by Nagel et al. [29]. Muramatsu et al. [30] showed that $V_{FV,Ps}$ can satisfactorily describe the variation of O_2 permeability in both dry and hydrated ethylene vinyl alcohol copolymer (EVOH). Sodaye et al. [31,32] reported the free volume in H^+ and ion-exchanged forms of a Nafion sample with a brief discussion on O_2 diffusivity of the H^+ form. The same authors studied the temperature dependence of free volume in Nafion [33]. The aim of this work is to study the free volume in dry and hydrated Nafion by the PAL technique and relate it to O_2 and H_2 permeabilities. Further we discuss the mechanism of gas permeation based on the correlations between the permeabilities and $V_{FV,Ps}$.

2. Free volume theory of gas permeation in polymers

According to the sorption–diffusion model, gas permeation coefficient P is given as the product of permeant solubility S and diffusion coefficient D [12],

$$P = SD. \quad (3)$$

The permeant can diffuse when it finds large enough free volume around itself to make a jump to one of the neighboring sites. Therefore, the diffusivity can be related to the fractional free volume V_f by [34–36]

$$D = ART\exp\left(-B/V_f\right), \quad (4)$$

where A and B are constants depending on the permeant, R is the gas constant and T is the absolute temperature. Combination of Eq. (3) with Eq. (4) yields the following relationship between the permeability and free volume.

$$P = SART\exp\left(-B/V_f\right). \quad (5)$$

To correlate the free volume obtained by the PAL technique to gas diffusivity and permeability, the following equations have been proposed by replacing V_f in Eqs. (4) and (5) with $V_{FV,Ps}$

$$D = ART\exp\left(-b/V_{FV,PS}\right), \quad (6)$$

$$P = SART\exp\left(-b/V_{FV,Ps}\right), \\ = CT\exp\left(-b/V_{FV,Ps}\right). \quad (7)$$

According to the elaborated free volume model of Vrentas and Vrentas [37], b can be expressed as

$$b = \gamma V_1(0)/N_o M_j, \quad (8)$$

where γ is a free volume overlap factor of the order of 0.5 and $V_1(0)$ is the molecular gas volume at 0 K, M_j is the magnitude of the polymer jump unit, and N_o is the number density of holes. Eqs. (6) and (7) with an assumption of constant C have been quite successful for various polymers [28–30].

3. Experimental

A 50 μm thick Nafion film (NRE212) with ionic exchange capacity (IEC) = 0.92 meq/g and 50 μm thick films recast at 90 °C from 20% solutions of Nafion DE2021 and DE2020 with IEC = 0.92 and 1.00 meq/g, respectively, were used in the present study. The NRE212 film and solutions for recasting were received from DuPont Fuel Cells, Japan. For the as-received sample a peak around $q = 0.55$ nm^{-1} attributed to the long spacing in crystalline domains was clearly observed by small angle X-ray scattering (SAXS), where $q = (4\pi/\lambda)\sin\theta$ with the scattering angle 2θ and X-ray wavelength λ. No such peak was observed for a recast sample indicating its amorphous structure. All the three samples were used for the study of free volume and O_2 and H_2 permeabilities in the dry state as a function of temperature. We used NRE212 for the study of water uptake, free volume and O_2 permeability as a function of relative humidity.

Positron annihilation lifetime (PAL) measurements were performed using a conventional fast–fast coincidence system [38–40]. A positron source (^{22}Na), sealed in a thin foil of Kapton, was mounted in a sample (stack of films with a total thickness of 1 mm) – source–sample sandwich. The time resolution of the system was 280 ps (full width at half maximum, FWHM). The PAL spectra containing 2.5×10^6 counts were analyzed using the PALSfit program [41] into three components to deduce lifetime τ_3 and intensity I_3.

Temperature dependence of free volume was measured by cooling the samples from 80 to −60 °C and then heating them from −55 to 75 °C with a step of 10° under vacuum. Before the measurements, we dried all the samples by evacuation for 1 day at room temperature (~25 °C) and then maintaining them at 80 °C for 10 h under vacuum. To study the effect of humidity on the free volume the sample was placed inside a glass container with temperature controlled to 25 °C and relative humidity controlled between 0 and 100% by adjusting the flowing rate ratio of water saturated wet N_2 to dry N_2. The relative humidity was measured using a high-accuracy humidity sensor. The PAL measurements were repeatedly performed until the *o*-Ps parameters for the equilibrium state in the given relative humidity were obtained.

Water uptake was measured by an MSB-AD-V-FC isothermal absorption measurement system (BEL Japan Inc.) equipped with a magnetically floating balance. The membrane was cut into strips of 2.5 cm wide and 4.0 cm long, put in the balance basket, and then placed in a stainless steel chamber, where the temperature and humidity were controlled by flowing N_2 humidified to 0–95% relative humidity at 40 °C. After the membrane was equilibrated with the humidified gas for at least 3 h, then the sample weight was measured and the water uptake was calculated in wt.% as

$(W_w/W_d - 1)100$, where W_w is the weight of the wet membrane and W_d is that of the membrane in the dry state.

Gas permeabilities were measured with a GTR-Tech 30XFST apparatus equipped with a Yanaco G2700T gas chromatograph by monitoring the amounts of O_2 and H_2 that permeated across the membrane from one side to the other. Temperature dependence of the permeation coefficients P of O_2 and H_2 was measured from −30 to 80 °C, whereas the humidity dependence of P was measured for O_2 at 30 °C. Ar and He were used as carrier gases of H_2 and O_2, respectively. A 50 μm thick membrane was set in a cell that had a gas inlet and outlet, where the temperature was controlled. Both H_2 and O_2 were supplied at a flow rate of 30 mL/min.

4. Results

4.1. Free volume and gas permeabilities under a dry condition

Table 1 lists the *o*-Ps lifetime τ_3, its intensity I_3, and free volume hole size $V_{FV,Ps}$ of dry NRE212, DE2021, and DE2020 at 30 °C, along with the corresponding data of polytetrafluoroethylene (PTFE). The free volume sizes for the Nafion samples with IEC = 0.92–1.00 meq/g are ranged from 0.163 to 0.191 nm^3 and much smaller than PTFE with IEC = 0 meq/g (0.297 nm^3). The difference may be due to the attractive interaction between the polar sulfonate groups, making free volume in Nafion smaller than nonpolar PTFE. The *o*-Ps intensity of Nafion is smaller by a factor of 3 than PTFE, indicating that the polar groups considerably suppress positronium formation [42].

Fig. 2 shows temperature dependence of the *o*-Ps lifetime τ_3 for dry NRE212, DE2021 and DE2020. The *o*-Ps relative intensity I_3 (data not shown) varies only slightly with temperature, indicating that positronium formation does not significantly depend on temperature. The right hand ordinate of Fig. 2 represents the free volume hole size quantified by Eqs. (1) and (2). It is seen that the free volume of all the samples is considerably enlarged by thermal expansion. For example, the free volume of NRE212 expands from 0.117 to 0.255 nm^3 over the temperature range studied. Both heating and cooling scans show an abrupt change of the thermal expansion coefficient of the free volume around 20 °C, which may be attributed to β-transition caused by the glass transition of Nafion. According to Osborn et al. [43], this glass transition of H^+ form Nafion is attributed to principally main-chain (backbone) motions within the framework of a static physically cross-linked (hydrogen-bonding) network. The β-transition temperature is between −20 and 20 °C depending on the water uptake [1,43]. It is interesting to note that DE2020 with higher IEC and smaller free volume than the other samples exhibits a higher transition temperature. The larger slope above the β-transition temperature for all the samples suggests that the backbone segmental motions significantly contribute to the free volume at high temperatures.

Fig. 3 shows the temperature dependence of O_2 and H_2 permeabilities of dry NRE212, DE2021 and DE2020. It is seen that both O_2 and H_2 permeabilities increase by orders of magnitudes with increasing temperature from −30 to 80 °C. At all the temperatures studied, H_2 is much more permeable than O_2. Although all the samples show similar tendency in H_2 permeation, NRE212 exhibits a different behavior in O_2 permeation from the other two samples (DE2021 and DE2020) that were recast from solutions at 90 °C. This observation may be important to those studying polymer electrolyte fuel cells because recast films from dispersions are used to form the catalytic layer with carbon/Pt.

Table 1
The *o*-Ps lifetime, its intensity, and free volume hole size obtained by Eqs. (1) and (2) for dry NRE212, DE2021, DE2020, and PTFE at 30 °C

Samples	*o*-Ps lifetime τ_3 (ns)	*o*-Ps intensity I_3 (%)	Free volume hole size $V_{FV,PS}$ (nm^3)
PTFE (IEC = 0 meq/g)	3.83 ± 0.01	19.43 ± 0.05	0.297 ± 0.001
NRE212 (IEC = 0.92 meq/g)	2.77 ± 0.03	6.35 ± 0.07	0.175 ± 0.001
DE2021 (IEC = 0.92 meq/g)	2.92 ± 0.03	6.80 ± 0.06	0.191 ± 0.001
DE2020 (IEC = 1.00 meq/g)	2.66 ± 0.03	7.04 ± 0.09	0.163 ± 0.001

The uncertainties take account of those due to counting statistics. The PTFE sample was from Goodfellow (FP301400/5). The PTFE data are consistent with the recent report by Dlubek et al. [44].

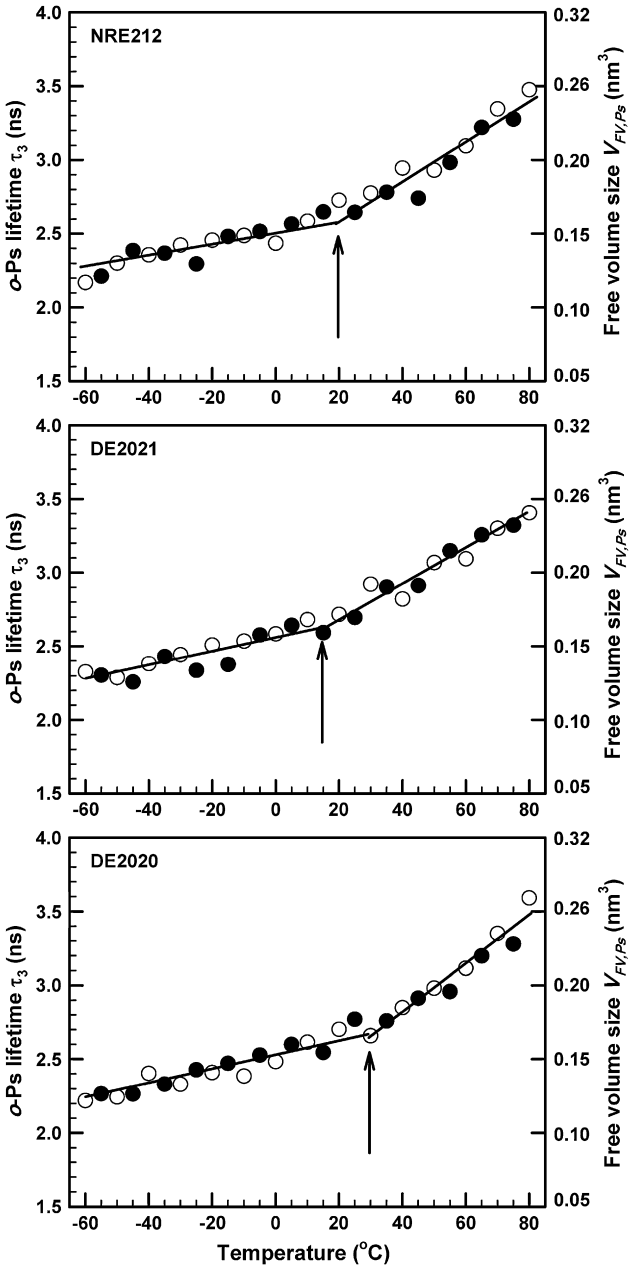

Fig. 2. The *o*-Ps lifetime τ_3 as a function of temperature for NRE212, DE2021, and DE2020. The scale of the right ordinate is the size of the hole deduced from Eqs. (1) and (2). ○: Cooling run, •: heating run.

4.2. Water uptake, free volume and O_2 permeability as a function of relative humidity

Variation of water uptake by dried NRE212 with relative humidity at 40 °C is shown in Fig. 4. These data are in good agreement with those of Zawodzinski et al. [7] for Nafion-117 at 30 °C. From

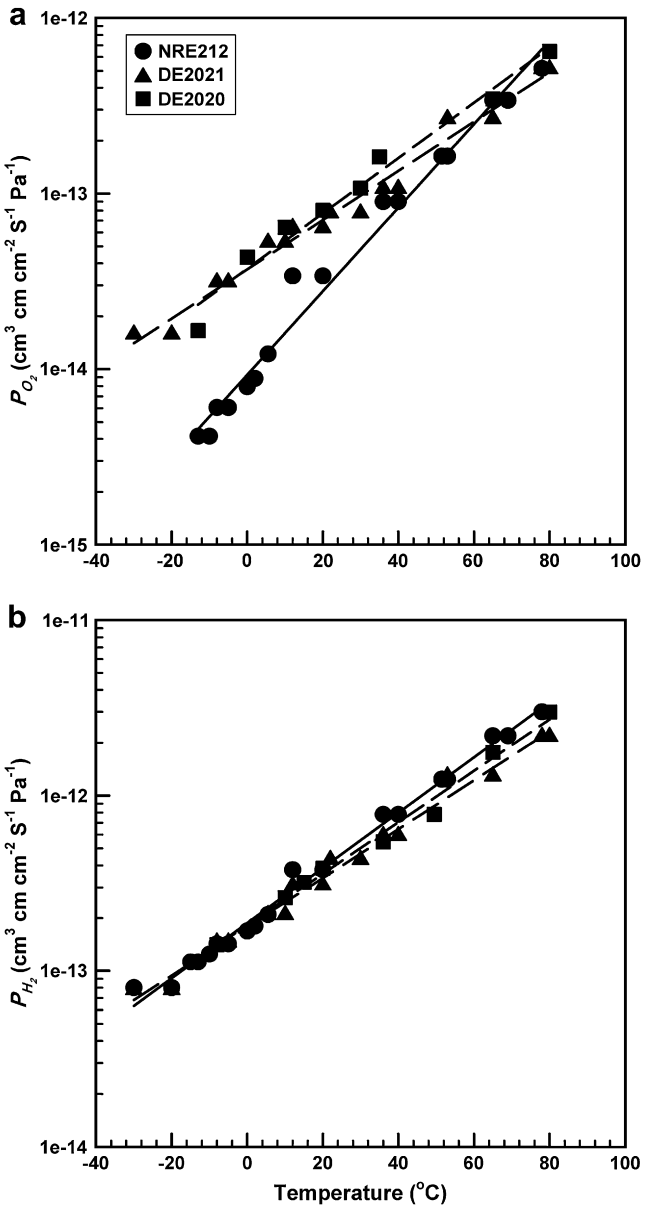

Fig. 3. Permeabilities of (A) O_2 and (B) H_2 as a function of temperature for dried NRE212, DE2021, and DE2020. The straight lines are drawn just for guiding the eyes.

these results, two different regions of water uptake may be discerned: (I) a region of relative humidity up to 60%, where water content increases only slightly with increasing relative humidity and (II) a region of relative humidity above 60%, where a sharp increase of water content is seen. Region I corresponds to uptake of water of solvation of the proton and sulfonate ions. Here, the water in the polymer is engaged in strong interactions with the ionic components of the polymer, which overcome the strong tendency of the polymer to exclude water due to its hydrophobic nature and resistance to swelling. In region II, the hindrance to uptake water is surmounted since the water in the bathing gas has sufficient chemical potential [7].

The *o*-Ps lifetime τ_3 and free volume hole size $V_{FV,Ps}$ in NRE212 at 25 °C are shown in Fig. 5 as a function of relative humidity. The *o*-Ps relative intensity I_3 (data not shown) only slightly changes with relative humidity. In region I, the free volume is essentially unchanged with relative humidity up to 20%, beyond which there is a significant increase in the free volume size. In region II (above 60% relative humidity), the free volume size decreases gradually with increasing relative humidity.

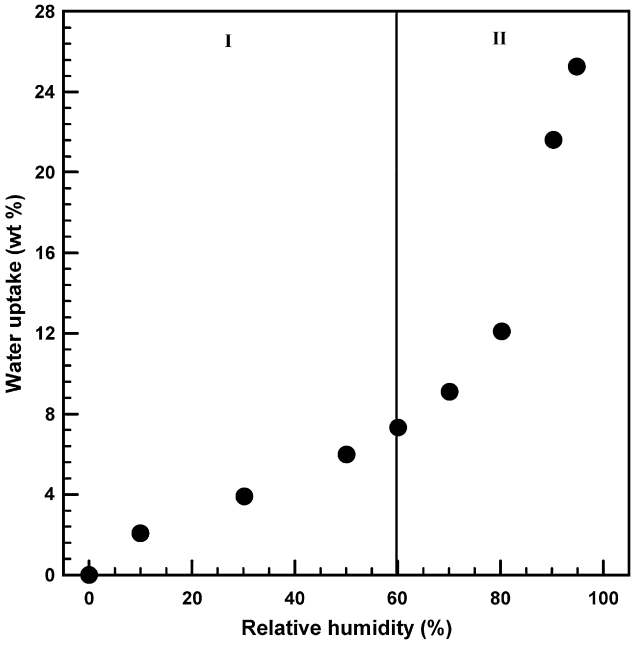

Fig. 4. Water uptake at 40 °C as a function of relative humidity for NRE212.

Fig. 6 displays the change of the O_2 permeation coefficient in NRE212 with relative humidity. The permeability increases substantially, by a factor of about 5, with increasing the relative humidity from 0 to 25%. In the range between 25 and 90% relative humidity it gradually increases as a function of relative humidity.

5. Discussion

5.1. Free volume in Nafion probed by the PAL technique

Previous studies of various polymers by the PAL technique revealed that the free volume is influenced by temperature and molecular motions associated with various transitions [45–48]. We

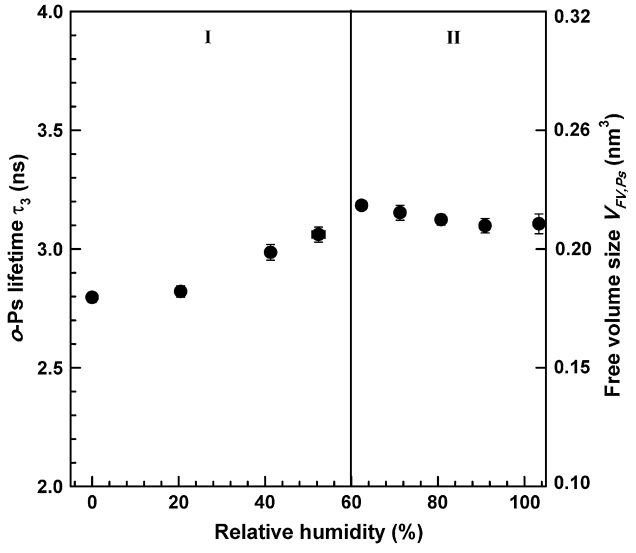

Fig. 5. The *o*-Ps lifetime τ_3 at 25 °C as a function of relative humidity for NRE212. The scale of the right ordinate is the size of the hole deduced from Eqs. (1) and (2).

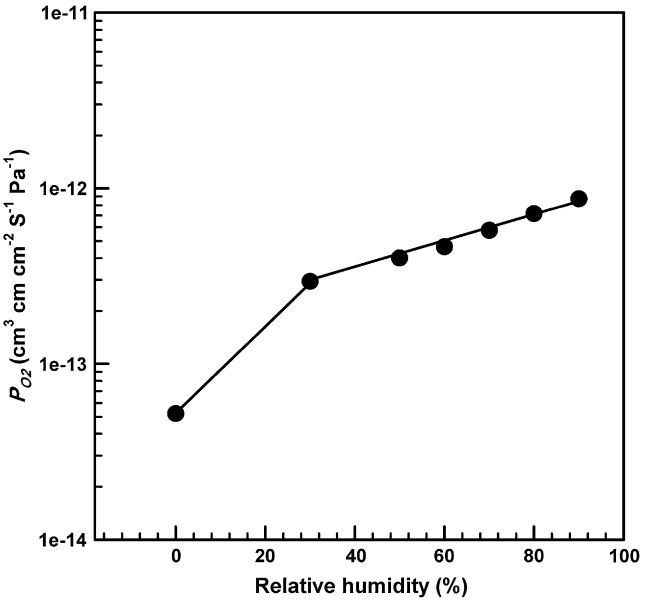

Fig. 6. Permeability of O_2 as a function of relative humidity for NRE212.

confirmed that this is also the case for dry Nafion from the results shown in Fig. 2. The effect of IEC summarized in Table 1 is also understandable by the attractive interaction between the polar sulfonate groups, which makes the interchain spacing in the amorphous region smaller in comparison with nonpolar PTFE. However, the humidity dependence of the free volume in Fig. 5 is more complicated and requires further discussion.

Muramatsu et al. [30] studied the free volume in EVOH as a function of relative humidity by the PAL technique. A shallow dip in free volume size was observed around 30% relative humidity, which was attributed to the filling of preexisting free volume by water molecules. At higher relative humidity, where a larger amount of water was absorbed, free volume was enlarged due to the plasticization of EVOH by water. The above results agree with the molecular dynamics (MD) simulation of poly(methyl methacrylate) (PMMA) containing water at high temperatures [49], which showed that the fractional free volume is reduced by a small amount of water but is enhanced when the water content exceeds 3 wt.%. It was also shown that the diffusion coefficient of N_2 can be well correlated to fractional free volume V_f by Eq. (4) [49].

Our results of NRE212 for region I are similar to the previous data for EVOH and PMMA [30,49]; the larger water uptake at higher relative humidity results in significant increase of free volume. In the case of Nafion this could be attributed to the plasticization effect of water in the ionic clusters. However, the observed decrease of the free volume in region II is unexpectedly different from the previous data for EVOH and PMMA. The gradual decrease of the free volume with relative humidity may be a result of more positronium annihilating in the aqueous phase due to large uptake of water. The lifetime of *o*-Ps in pure water is approximately 1.8 ns [24] corresponding to smaller free volume than in dry Nafion.

5.2. Correlations between permeability and free volume

Fig. 7 shows the plot of P/T versus $1/V_{FV,Ps}$ for the permeation of O_2 and H_2 in dried NRE212, DE2021, and DE2020 at various temperatures. Reasonably good correlations in line with Eq. (7) are observed, indicating that the free volume governs the gas permeation in Nafion as in other polymers. Also included in this figure is a plot of O_2 permeability for relatively flexible chain polymers

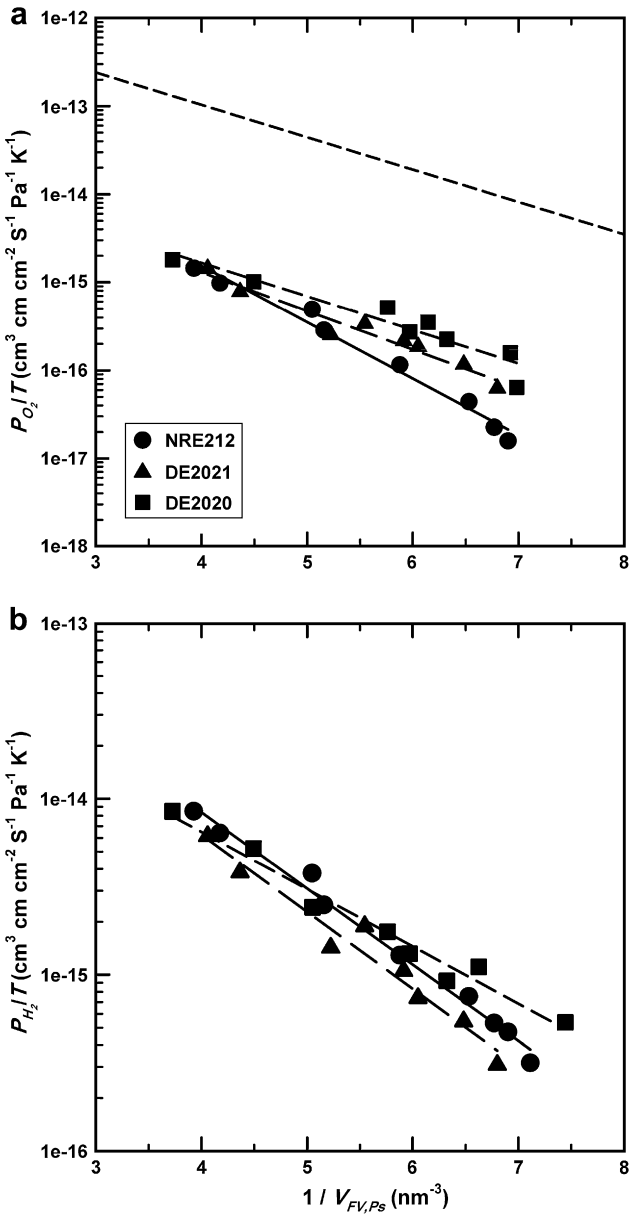

Fig. 7. Correlation between the permeabilities of (A) O_2 and (B) H_2 and reciprocal free volume hole size for dry samples at different temperatures. The small dashed line in (A) shows the correlation for relatively flexible chain polymers such as polydimethylsiloxane, polystyrene, polysulfone, polyethersulfone, EVOH, etc. [30].

reported by Muramatsu et al. [30]. Comparison of our data with this plot reveals much smaller O_2 permeability in Nafion for a particular size of free volume. Similar tendency was observed for O_2 and N_2 diffusion coefficients in fluorinated poly(amide imide), poly(ester imide) and polyimide [29,36]. The latter polymers are those of more stiff chains than the former with flexible backbones or of short building blocks coupled by a flexible ether link. The present considerations indicate that dry Nafion behaves as a stiff chain polymer in its O_2 permeation, which presumably originates from the presence of the backbone containing a number of fluorine atoms covalently bonded to a carbon atom. The arguments involving stiff chains in dry Nafion are in agreement with the recent NMR work of Chen and Schmidt-Rohr [50], according to which this backbone stiffness can be attributed at least in part to the steric crowding of fluorine atoms, which are larger than the hydrogen atoms, for example, in polyethylene.

Table 2
C and *b* parameters for O_2 and H_2 permeation in different samples

Samples	*C* ($cm^3\,cm\,cm^{-2}\,S^{-1}\,Pa^{-1}\,K^{-1}$)		*b* (nm^3)	
	O_2	H_2	O_2	H_2
NRE212	5.8×10^{-13}	4.5×10^{-13}	0.64	0.43
DE2021	7.5×10^{-14}	3.5×10^{-13}	0.44	0.44
DE2020	5.7×10^{-14}	1.3×10^{-13}	0.38	0.33

The *C* and *b* parameters obtained by fitting our data to Eq. (7) are listed in Table 2. The lower values of *b* for H_2 than O_2 are reasonable in view of Eq. (8) and the smaller size ($V_1(0)$) of the H_2 molecule. The diffusion of H_2 should be more of the interstitial type and its diffusion can occur without major free volume fluctuations [29,36]. The difference of the *C* and *b* parameters between the as-received and recast samples, in particular, for O_2 permeation may be due to their different crystallinities. Both the parameters of as-received NRE212 for O_2 permeation are appreciably larger than the other samples that were recast from solutions. IEC plays a minor role because the parameters are similar to each other between DE2021 and DE2020. Lee et al. [51] reported that the recast temperature and crystallinity for the preparation of Nafion film have significant impacts on its morphology and O_2 permeation. The larger *b* for the as-received sample indicates that the crystallinity enhances the minimum free volume required for O_2 diffusion. The different *C* values between the as-received and recast samples could be related to different O_2 solubilities [51].

The plot of P/T versus $1/V_{FV,Ps}$ for the permeation of O_2 in NRE212 at different relative humidities is shown in Fig. 8. At low relative humidities the tendency is analogous to that in the temperature dependence of dry Nafion; the permeability is governed by free volume $V_{FV,Ps}$ but limited by stiff chains. Between 50 and 60% relative humidities the permeability depends less on free volume possibly due to reduced solubility [52]. At 60% relative humidity it starts increasing with decreasing free volume as opposed to the free volume theory of permeation. Then the data point moves toward the upper-right direction and gradually approaches the correlation for EVOH, indicative of a transition from the stiff chain to flexible chain behavior. This is consistent with the data in Figs. 4 and 5 suggesting the abrupt change of the state and interaction of water in Nafion at 60% relative humidity. We consider that large uptake of water itself and its interaction with the side chains in the amorphous region enhance the overall flexibility of hydrated Nafion. There is some evidence by nuclear magnetic resonance (NMR) that the absorbed water increases the segmental mobility of Nafion [50]. Interestingly, not only the side chains but also backbones show additional motional narrowing of the NMR spectrum in the wet sample. Therefore in highly hydrated Nafion (above 60% relative humidity) gas permeation is controlled by molecular motions but not by free volume.

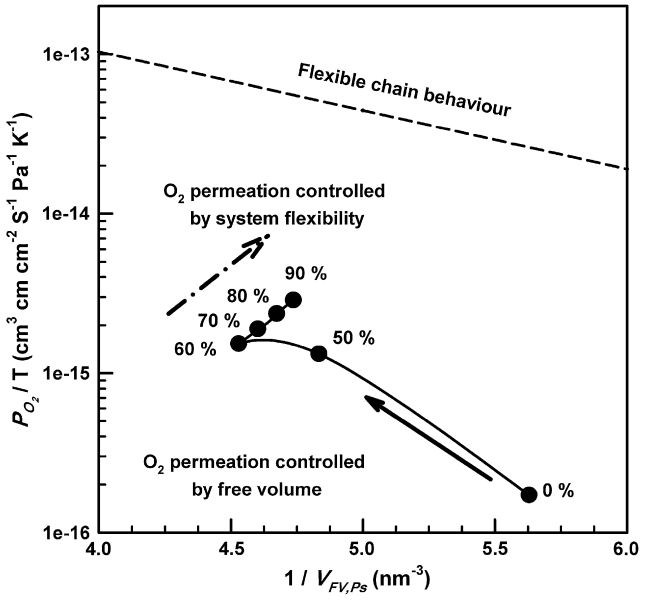

Fig. 8. Correlation between the permeability of O_2 and reciprocal free volume hole size for NRE212 at different relative humidities. The small dashed line shows the correlation for EVOH with flexible chains [30].

6. Conclusion

We studied free volume and gas permeation in dry and hydrated Nafion at various temperatures and relative humidities. Free volume was evaluated from the *o*-Ps lifetimes and gas permeabilities were measured for O_2 and H_2. As evidenced by good correlations between the permeabilities and free volume, we concluded that the free volume governs gas permeation in dry and weakly hydrated Nafion similarly to other polymers. Comparison of the result with available data for relatively flexible chain polymers showed that the stiff chains of the perfluoroethylene backbone in Nafion make the O_2 permeability much smaller than the corresponding flexible chain polymer with a similar free volume size. In highly hydrated Nafion above 60% relative humidity, where the O_2 permeability increases with the decrease of the free volume size, gas permeation proved to be controlled by the enhancement of molecular motions due to larger water uptake.

Acknowledgement

One of the authors (Hamdy F.M. Mohamed) is grateful to Arab Foundation for the fellowship, which makes his stay in Japan possible. Thanks are extended to Drs. C. He and T. Oka for enlightening discussions. This work was supported by the Ministry of Economy, Trade and Industry, Japan.

References

[1] Mauritz KA, Moore RB. Chem Rev 2004;104:4535–85.
[2] Gierke TD, Munn GE, Wilson FC. J Polym Sci Part B Polym Phys 1981;19:1687–704.
[3] Schmidt-Rohr K, Chen QS. Nat Mater 2008;7:75–83.
[4] Eisenberg A. Macromolecules 1970;3:147–54.
[5] Xue T, Trent JS, Osseo-Asare K. J Membr Sci 1989;45:261–71.
[6] Lee EM, Thomas RK, Burgess AN, Barnes DJ, Soper AK, Rennie AR. Macromolecules 1992;25:3106–9.
[7] Zawodzinski TA, Derouin C, Radzinski S, Sherman RJ, Smith VT, Springer TE, et al. J Electrochem Soc 1993;140:1041–7.
[8] Buchi FN, Wakizoe M, Srinivasan S. J Electrochem Soc 1996;143:927–32.
[9] Ogumi Z, Takehara Z, Yoshizawa S. J Electrochem Soc 1984;131:769–73.
[10] Ogumi Z, Kuroe T, Takehara Z. J Electrochem Soc 1985;132:2601–5.
[11] Tsou Y, Kimble MC, White RE. J Electrochem Soc 1992;139:1913–7.
[12] Vegt AK. From polymers to plastics. The Netherlands: Delft University Press; 2002. p. 159.
[13] Yampolskii YP. Uspekhi Khimii 2007;76:66–87.
[14] Oka T, Ito K, Muramatsu M, Ohdaira T, Suzuki R, Kobayashi Y. J Phys Chem B 2006;110:20172–6.
[15] Soles CL, Douglas JF, Wu W, Peng H, Gidley DW. Macromolecules 2004;37:2890–900.
[16] Ito K, Oka T, Kobayashi Y, Suzuki R, Ohdaira T. Radiat Phys Chem 2007;76:213–6.
[17] Mohamed HFM, Abdel-Hady EE, Mohamed SS. Radiat Phys Chem 2007;76:160–4.
[18] Abdel-Hady EE, Abdel-Hamid HM, Mohamed HFM. Radiat Meas 2004;38:211–6.
[19] Kobayashi Y, Zheng W, Meyer EF, McGervey JD, Jamieson AM, Simha R. Macromolecules 1989;22:2302–6.
[20] Ito K, Saito Y, Yamamoto T, Ujihira Y, Nomura K. Macromolecules 2001;34:6153–5.
[21] Schmidt M, Maurer FHJ. Macromolecules 2000;33:3879–91.
[22] Wästlund C, Maurer FHJ. Macromolecules 1997;30:5870–6.

[23] Winberg P, DeSitter K, Dotremont C, Mullens S, Vankelecom IFJ, Maurer FHJ. Macromolecules 2005;38:3776–82.
[24] Schrader DM, Jean YC. Positron and positronium chemistry. Amsterdam: Elsevier; 1988.
[25] Tao SJ. J Chem Phys 1972;56:5499–510.
[26] Eldrup M, Lightbody D, Sherwood JN. Chem Phys 1981;63:51–8.
[27] Nakanishi H, Wang SJ, Jean YC. In: Sharama SC, editor. Positron annihilation studies of fluids. Singapore: World Scientific; 1988. p. 292–8.
[28] Kobayashi Y, Haraya K, Hattori S, Sasuga T. Polymer 1994;35:925–8.
[29] Nagel C, Günther-Schade K, Fritsch D, Strunskus T, Faupel F. Macromolecules 2002;35:2071–7.
[30] Muramatsu M, Okura M, Kuboyama K, Ougizawa T, Yamamoto T, Nishihara Y, et al. Radiat Phys Chem 2003;68:561–4.
[31] Sodaye HS, Pujari PK, Goswami A, Manohar SB. J Polym Sci Part B Polym Phys 1997;35:771–6.
[32] Sodaye HS, Pujari PK, Goswami A, Manohar SB. J Polym Sci Part B Polym Phys 1998;36:983–9.
[33] Sodaye HS, Pujari PK, Goswami A, Manohar SB. Radiat Phys Chem 2000;58:567–70.
[34] Cohen MH, Turnbull D. J Chem Phys 1959;31:1164–9.
[35] Fujita H. Fortschr Hochpolym Forsch 1961;3:1–47.
[36] Thran A, Kroll G, Faupel F. J Polym Sci Part B Polym Phys 1999;37:3344–58.
[37] Vrentas JS, Vrentas CM. J Polym Sci Part B Polym Phys 1993;31:69–76.
[38] Wang CL, Hirata K, Kawahara J, Kobayashi Y. Phys Rev B 1998;58:14864–9.
[39] Kobayashi Y, Wang CL, Hirata K, Zheng W, Zhang C. Phys Rev B 1998;58:5384–9.
[40] Saddeek YB, Mohamed HFM, Azooz MA. Phys Stat Sol A 2004;201:2053–62.
[41] Olsen JV, Kirkegaard P, Pedersen NJ, Eldrup M. Risø National Laboratory, Denmark; 2007.
[42] Mogenson OE. Positron annihilation in chemistry. Berlin, Heidelberg, Germany: Springer-Verlag; 1995.
[43] Osborn SJ, Hassan MK, Divoux GM, Rhoades DW, Mauritz KA, Moore RB. Macromolecules 2007;40:3886–90.
[44] Dlubek G, Gupta AS, Pionteck J, HaBler R, Krause-Rehberg R, Kaspar H, et al. Polymer 2005;46:6075–89.
[45] Hagiwara K, Ougizawa T, Inoue T, Hirata K, Kobayashi Y. Mater Sci Forum 2001;363–365:337–9.
[46] Abdel-Hady EE, Mohamed HFM. Polym Degrad Stab 2002;77:449–56.
[47] Hagiwara K, Ougizawa T, Inoue T, Hirata K, Kobayashi Y. Radiat Phys Chem 2000;58:525–30.
[48] Mohamed HFM, Abdel-Hady EE, Alaa HB. Mater Sci Forum 2004;445–446:328–30.
[49] Bharadwaj RK. Macromolecules 2002;35:5334–6.
[50] Chen QS, Schmidt-Rohr K. Macromol Chem Phys 2007;208:2189–203.
[51] Lee K, Ishihara A, Mitsushima S, Kamiya N, Ota K. J Electrochem Soc 2004;151:A639–45.
[52] Gode P, Lindbergh G, Sundholm G. J Electroanal Chem 2002;518:115–22.